Journal of the American College of Cardiology Vol. 47, No. 8 Suppl C

Published by Elsevier Inc.
ISSN 0735-1097/06/$32.00
doi:10.1016/j.jacc.2006.01.035

Intravascular Palpography for Vulnerable Plaque Assessment

Johannes A. Schaar, MD,*† Anton F. W. van der Steen, PHD,*† Frits Mastik,* Radj A. Baldewsing, MSC,* Patrick W. Serruys, MD, PHD*

Rotterdam and Utrecht, the Netherlands

Palpography assesses the local mechanical properties of tissue using the deformation caused by the intraluminal pressure. The technique was validated in vitro using diseased human coronary and femoral arteries. Especially between fibrous and fatty tissue, a highly significant difference in strain ($p = 0.0012$) was found. Additionally, the predictive value to identify the vulnerable plaque was investigated. A high-strain region at the lumen vessel wall boundary has 88% sensitivity and 89% specificity for identifying these plaques. In vivo, the technique is validated in an atherosclerotic Yucatan minipig animal model. This study also revealed higher strain values in fatty than in fibrous plaques ($p < 0.001$). The presence of a high-strain region at the lumen-plaque interface has a high predictive value to identify macrophages. Patient studies revealed high strain values (1% to 2%) in noncalcified plaques. Calcified material showed low strain values (0% to 0.2%). With the development of three-dimensional palpography, identification of weak spots over the full length of a coronary artery becomes available. Patients with myocardial infarction or unstable angina have more high-strain spots in their coronary arteries than patients with stable angina. In conclusion, intravascular palpography is a unique tool to assess lesion composition and vulnerability. Three-dimensional palpography provides a technique that may develop into a clinically available tool for decision making to treat hemodynamically nonsignificant lesions by identifying vulnerable plaques. The clinical utility of this technique is yet to be determined, and more investigation is needed. (J Am Coll Cardiol 2006;47:C86–91) © 2006 by the American College of Cardiology Foundation

For the detection of vulnerable plaque, it is important to identify not only the composition and geometry of the plaques but also the response of the tissue to the pulsating force applied by the blood pressure. The plaque is supposed to be rupture prone if the cap is unable to withstand the stress applied on it. All the stress that is applied on the plaque by the blood pressure is concentrated in the cap, because the lipid pool is unable to withstand forces on it (1,2). During plaque development, the stress in the cap can further increase when: 1) caps become thinner; 2) lipid pools become larger; or 3) the difference in stiffness between the cap and the lipid pool increases. Furthermore, the strength of the cap is affected by inflammation: Fibrous caps with inflammation by macrophages were locally weakened (3). Therefore, the strength of a cap seems to be a more important parameter than the thickness of a cap.

The local relation between stress and strain in an artery is, approximately, as follows (4): The ratio of circumferential tensile stress to the radial strain equals the stiffness of the tissue. This stress-strain relation implies that an increase in circumferential stress will give an increase in radial strain. This strain is assessed with intravascular palpography, which is based on intravascular ultrasound (IVUS). Intravascular ultrasound is the only commercially available clinical technique providing a real-time cross-sectional image of the coronary artery (5). Using IVUS, detailed information of the coronary wall and plaque can be obtained. Furthermore, calcified and noncalcified plaque components can be identified. However, the sensitivity to identify fatty plaque components remains low (6,7). Recent radiofrequency (RF)-based tissue identification strategies appear to have a better performance (7,8). With palpography, the local strain of the tissue is obtained. This strain is directly related to the mechanical properties of plaque components: Soft fatty tissue will be more strained than stiff fibrous tissue when equally stressed. Because the mechanical properties of fibrous and fatty plaque components are different (9–11), palpography has the potential to differentiate between different plaque components. An even more promising feature of palpography is the detection of high stress regions. Using computer simulations, concentrations of circumferential tensile stress were more frequently found in unstable plaque than in stable plaques (2,12). A local increase in circumferential stress in tissue is directly related to an increase in radial strain.

INTRAVASCULAR ELASTOGRAPHY AND PALPOGRAPHY

Céspedes et al. (13) and Ophir et al. (14) developed an imaging technique called elastography, which was based on tissue deformation. The rate of deformation (strain) of the tissue is directly related to the mechanical properties. The tissue under inspection is deformed and the strain between

From the *Thoraxcenter, Erasmus Medical Center, Rotterdam, and the †Interuniversity Cardiology Institute of the Netherlands, Utrecht, the Netherlands. Supported by the Dutch Technology Foundation, Netherlands Organization for Scientific Research, Dutch Heart Foundation, and German Heart Foundation. Dr. William A. Zoghbi acted as guest editor.

Manuscript received June 17, 2005; revised manuscript received December 9, 2005, accepted December 9, 2005.

Abbreviations and Acronyms

2D = two-dimensional
3D = three-dimensional
AMI = acute myocardial infarction
IVUS = intravascular ultrasound
RF = radiofrequency
SMC = smooth muscle cells

pairs of ultrasound signals before and after deformation is determined (15). For intravascular purposes, the compression can be obtained from the pressure difference in the artery. Additionally, well-controlled deformation is possible by using a compliant intravascular balloon (16).

The principle of intravascular elastography is illustrated in Figure 1. An ultrasound image of a human coronary artery is acquired at an intracoronary pressure. A second acquisition at a slightly lower pressure (~3 mm Hg) is performed. The strain is determined by estimating displacement of the RF signals of the two IVUS images. The local displacement of the tissue is determined using cross-correlation analysis of the depth-gated RF signals. A cross-correlation function between two shifted RF signals will have its maximum at the displacement that will align these signals. For each angle, starting from the lumen boundary, the displacement of a layer (225 μm) of tissue is determined. Then the displacement of the next (225 μm) layer of tissue is determined. The strain of the tissue can be calculated by dividing the differential displacement (displacement of proximal layer − displacement of distal layer) by the distance between these two layers. When the strain is determined for multiple layers in depth, a color-coded two-dimensional (2D) image of the strain can be constructed. The elastogram (image of the radial strain) is plotted as a complimentary image to the IVUS image. The elastogram shows the presence of an eccentric region with increased strain values at the shoulders of the eccentric plaque. Because the acting force of the blood pressure is applied on the lumen boundary a surface-based assessment of the mechanical properties—called palpography—was developed assessing the first 450-μm layer, in contrast to elastography, which assesses the entire plaque. This robust technique is easier to interpret and is based on the same cross-correlation technique. Palpography derives mechanical information of the surface of the plaque, where the rupture may happen. This information is color-coded and superimposed on the IVUS image.

PLAQUE CHARACTERIZATION

In the first experiments, elastography was used for plaque characterization. In the transition phase from proof of the concept trials to clinical application, elastography was re-

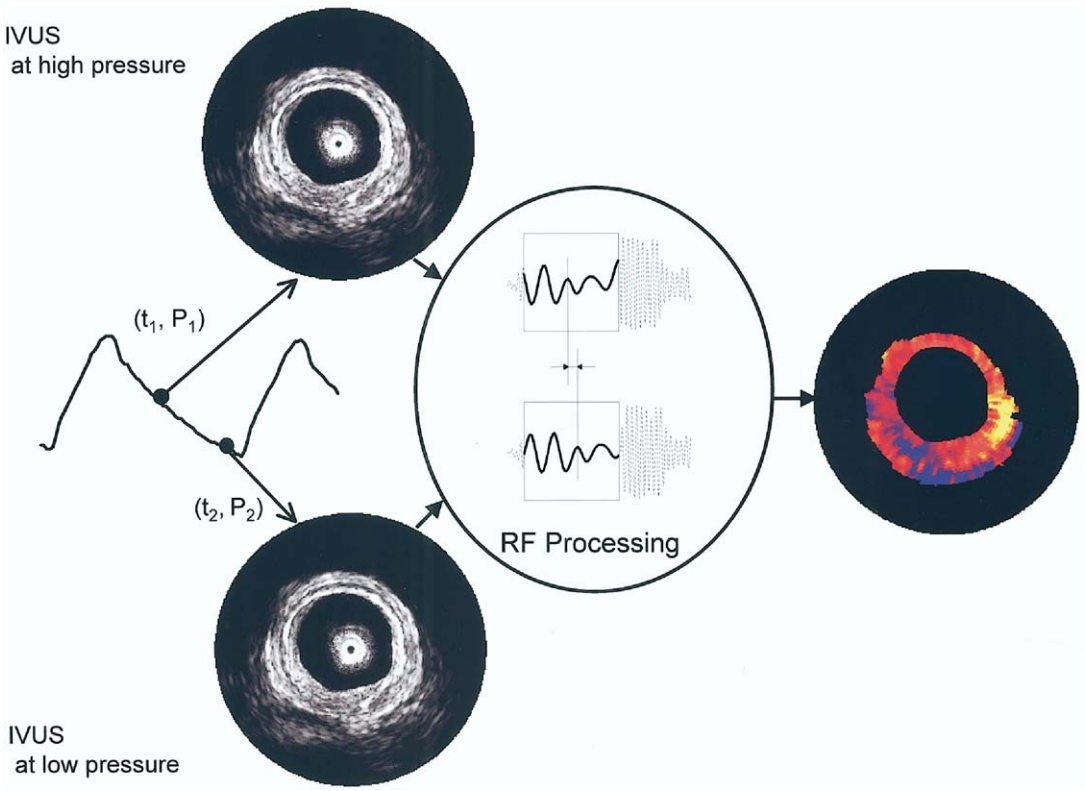

Figure 1. Principle of the intravascular elastography measurement procedure. An intravascular ultrasound (IVUS) image is acquired with a low (P_2) and a high (P_1) intraluminal pressure. Using cross-correlation analysis on the high-frequency radiofrequency data, the radial strain in the tissue is determined. This information is superimposed on the IVUS image. In this example, an eccentric soft lesion is visible between the 6- and 12-o'clock positions in the elastogram where it cannot be identified from the IVUS image.

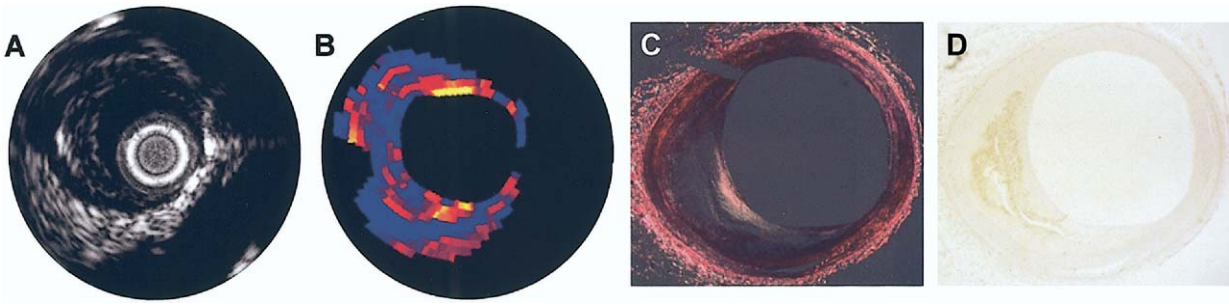

Figure 2. Intravascular ultrasound (IVUS) image **(A)** and elastogram **(B)** with corresponding histology of a coronary artery with a vulnerable plaque. The IVUS image reveals an eccentric plaque between the 6- and 12-o'clock positions. The elastogram shows high-strain regions **(yellow)** at the shoulders of the plaque surrounded by low-strain values **(blue)**. The histology reveals a plaque with a typical vulnerable appearance: A thin cap with a lack of collagen at the shoulders **(C)** and a large atheroma with heavy infiltration of macrophages **(D)**.

placed by palpography for the reasons mentioned in the preceding section.

Early elastographic experiments were performed in excised human coronary (n = 4) and femoral (n = 9) arteries (17). Data were acquired at room temperature at intraluminal pressures of 80 and 100 mm Hg. Coronary arteries were measured using a solid state 20-MHz array catheter (Volcano, Rancho Cordova, California). Femoral arteries were investigated using a single-element 30-MHz catheter (DuMed/EndoSonics, Rijswijk, the Netherlands). The RF data were stored. The processing is done off line. The visualized segments were stained for the presence of collagen, smooth muscle cells, and macrophages. Matching of elastographic data and histology was performed using the IVUS image. The cross sections were segmented in regions (n = 125) based on the strain value on the elastogram. The dominant plaque types in these regions (fibrous, fibrous/fatty, or fatty) were obtained from histology and correlated with the average strain and echo-intensity.

Mean strain values of 0.27 ± 0.16%, 0.45 ± 0.20%, and 0.60 ± 0.13% were found for fibrous, fibrous/fatty, and fatty plaque components, respectively. The strain for the three plaque types as determined by histology differed significantly ($p = 0.0002$). This difference was independent of the type of artery (coronary or femoral) and was mainly evident between fibrous and fatty tissue ($p = 0.0004$). The three different plaque types were statistically different, but an overlap of strain data was observed, which may be relevant to its potential clinical application for an individual patient or plaque. Using strain data and finite element modeling, the Young's modulus could be reconstructed. The Young's modulus is a physical material parameter. It indicates how much a material will deform under a given force. This may lead to a more precise tissue characterization. The plaque types did not reveal echo-intensity differences in the IVUS image ($p = 0.992$). Conversion of the strain into Young's modulus values resulted in 493 kPa, 296 kPa, and 222 kPa for fibrous, fibrous/fatty, and fatty plaques, respectively. Although these values are higher than values measured by Lee et al. (18), the ratio between fibrous and fatty material is similar. Because fibrous and fatty tissue demonstrated a different strain value, and high strain values were often colocalized with increased concentrations of macrophages, these results reveal the potential of identification of the vulnerable plaque features.

VULNERABLE PLAQUE DETECTION

Although plaque vulnerability is associated with the plaque composition, detection of a lipid or fibrous composition does not directly warrant identification of the vulnerable plaque. Therefore, a study to evaluate the predictive power of palpography to identify the vulnerable plaque was performed (19).

Diseased coronary arteries (n = 24) were measured in vitro. Palpographic data were acquired at intracoronary pressures of 80 and 100 mm Hg using a standard IVUS catheter (Volcano). After the ultrasound experiments, the cross sections were stained for collagen and fat, smooth muscle cells (SMCs), and macrophages. In histology, a vulnerable plaque was defined as a lesion with a large atheroma (>40%) and a thin fibrous cap with moderate to heavy infiltration of macrophages. A plaque was considered vulnerable in palpography when a high-strain region was present at the lumen-plaque boundary that was surrounded by low strain values. Using this definition, the instability of the region was assessed.

Figure 2 shows a typical example of a vulnerable plaque. High-strain regions are present at the 6- and 12-o'clock positions, and they are surrounded by low-strain values. These regions correspond to the shoulders of this eccentric plaque. The histology reveals a large lipid pool (absence of collagen and SMC) that is covered by a thin fibrous cap. The cap lacks collagen at the shoulder regions. Inflammation by macrophages is found in the lipid pool and in the cap.

In 24 diseased coronary arteries, we studied 54 cross sections. In histology, 26 vulnerable plaques and 28 nonvulnerable plaques were found. Palpography was positive in 23 cases but negative in 3 cases. Nonvulnerable plaques were seen by histology in 28 cases and detected by palpography in 25 cases and falsely diagnosed as positive in 3 cases, resulting in a sensitivity of 88% and a specificity of 89% to detect vulnerable plaques. Linear regression showed a high correlation between the strain in caps and the amount of

macrophages ($p < 0.006$) and an inverse relation between the amount of smooth muscle cells and strain ($p < 0.0001$). Plaques, which are declared vulnerable in palpography, have a thinner cap than nonvulnerable plaques ($p < 0.0001$) (19).

IN VIVO VALIDATION

Intravascular ultrasound palpography was validated in vivo using an atherosclerotic Yucatan minipig (20). External iliac and femoral arteries were made atherosclerotic by endothelial Fogarty denudation and a subsequent atherosclerotic diet for the duration of seven months. Balloon dilation was performed in the femoral arteries and the diet was discontinued. Before termination, six weeks after balloon dilation and discontinuation of the diet, data were acquired in the external iliac and femoral artery in six Yucatan pigs. In total, 20 cross sections were investigated with a 20-MHz Visions catheter (Volcano). The tissue was strained by the pulsatile blood pressure. Two frames acquired at end-diastole with a pressure differential of ~3 mm Hg were taken to determine the elastograms.

After the ultrasound experiments and before dissection, X-ray was used to identify the arterial segments that had been investigated by ultrasound. The specimens were frozen in liquid nitrogen. The cross sections (7 μm) were stained for collagen (picro Sirius red and polarized light) and macrophages (alcalic phosphatase). Plaques were classified as absent, early fibrous lesion, early fatty lesion, or advanced fibrous plaque. The mean strain in these plaques and normal cross-sections was determined to assess the tissue characterization properties of the technique. Furthermore, the deformability of the acquisition correlated with the presence of fat and macrophages. The deformability was characterized by the presence of a high-strain region (strain higher than 1%) at the lumen vessel-wall boundary.

Strains were similar in the plaque-free arterial wall and the early and advanced fibrous plaques. Univariate analysis of variance revealed significantly higher strain values in cross-sections with early fatty lesions than with fibrous plaques ($p = 0.02$) independently of the presence of macrophages. Although a higher strain value was found in plaques with macrophages than in plaques without macrophages, this difference was not significant after correction for fatty components. However, the presence of a high strain region had a high sensitivity (92%) and specificity (92%) to identify the presence of macrophages. Therefore, it was concluded that the tissue type dominates the mean strain value. Localized high strain values are related to local phenomena such as inflammation.

CLINICAL STUDIES

Preliminary acquisitions were performed in patients during percutaneous transluminal coronary angioplasty procedures (21). Data were acquired in patients ($n = 12$) with an ultrasound machine (InVision, Volcano) equipped with an analog RF output that was interfaced to a digitizer (Signatec, Corona, California). For obtaining the RF data, the machine was working in ChromaFlo mode resulting in images of 64 angles with unfocused ultrasound data. The systemic pressure was used to strain the tissue. This strain was determined using cross-correlation analysis of sequential frames. Because motion of the catheter prevents reliable strain estimation, recordings were done near end-diastole where minimal motion was observed. Reproducible strain estimates were obtained within one pressure cycle and over several pressure cycles. Validation of the results was limited to the information provided by the IVUS image. Strain in calcified material (0.20%) was lower ($p < 0.001$) than in noncalcified tissue (0.51%).

High-resolution elastograms were acquired using an ultrasound machine (InVision, Volcano) (22). The beam-formed image mode (512 angles) ultrasound digital RF data ($f_c = 20$ MHz) was acquired with a PC-based acquisition system. Frames acquired at end-diastole with a pressure difference of ~5 mm Hg were taken to determine the elastograms.

The palpogram of a patient with unstable angina pectoris reveals high strain values in the plaque with very high strain values (up to 2%) at the shoulders of this plaque (Fig. 3). This geometry and strain distribution was also found in the in vitro studies. The corresponding histology from in vitro studies revealed a plaque with a large lipid core covered from the blood by a thin cap. Calcified material, as identified from the IVUS image, shows strain values of 0% to 0.2%.

THREE-DIMENSIONAL (3D) PALPOGRAPHY: LIMITATIONS AND FUTURE DIRECTIONS

In the previous studies, elastograms revealed information on a 2D cross-section. However, the distribution of the strain in the 3D geometry of an artery is an important tool to identify the presence of high-strain spots, the amount, and the distribution. Especially because the correlation between plaque vulnerability and parameters provided by the IVUS image is low (6,7), selection of cross sections based on the IVUS image introduces selection bias and increases the chance of missing the vulnerable part. Additionally, during longitudinal monitoring of patients it is extremely difficult to find the same spot again after some months. Therefore, an acquisition method to get strain information of the full 3D coronary artery was developed. Because the rupture of a plaque happens in the superficial area of the plaque, the elastic information of the surface is displayed as the palpogram.

In palpography, out-of-plane motion is considered to be one of the main sources for decorrelation of the signals, thus decreasing the quality of the strain estimate (23,24). Therefore, for palpographic acquisitions the position of the transducer is kept as stable as possible and only motion in the direction of the beam is allowed. As a consequence, it is unlikely that valid intravascular strain palpograms can be obtained while performing a continuous pullback of

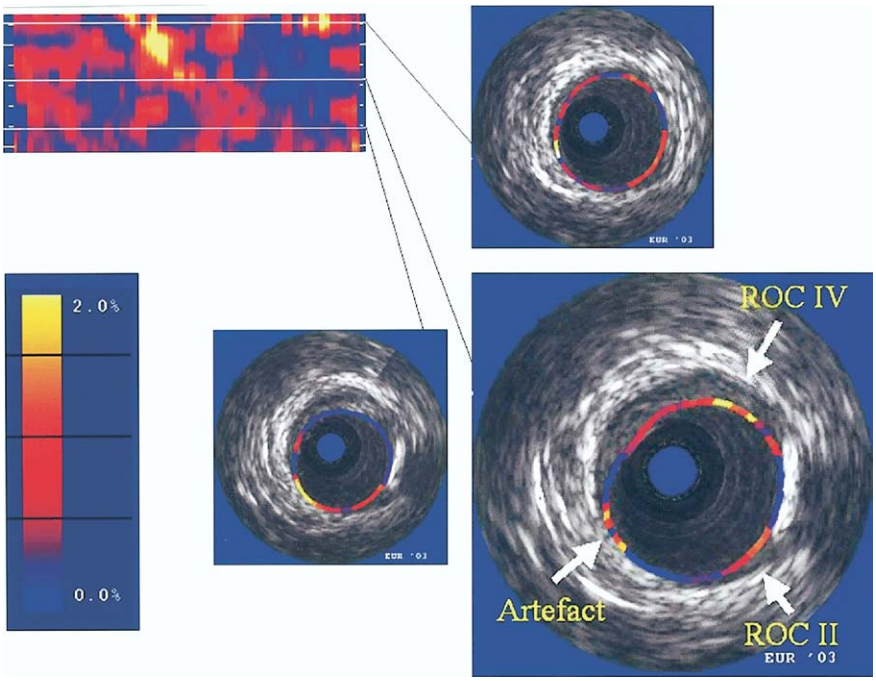

Figure 3. In vivo intravascular ultrasound image and palpogram of a human coronary artery. The elastogram reveals that the plaque has soft edges with adjacent hard (calcified) tissue. Plaque deformability was scored according to the Rotterdam classification (ROC), in which ROC I and IV indicate low (0% to 0.6%) and very high (>1.2%) deformation, respectively, by strain.

the catheter. However, if the pullback speed is slow and the strain is determined using two subsequent frames, the motion introduced by the pullback is minimal. Furthermore, it is known that, owing to the contraction of the heart, in diastole the catheter will move distally in the coronary artery if the catheter is kept at a steady position. Therefore, performing a pullback will decrease out-of-plane motion in this phase of the heart cycle. Because palpography uses data acquired in the diastolic phase, performing a pullback and thus obtaining 3D data seems feasible.

Preliminary experiments in rabbit aortas revealed that 3D palpography is feasible in vivo. Despite the introduction of out-of-plane motion by the continuous pullback of the catheter, the similarity between successive frames acquired in the diastolic phase is high enough to calculate several palpograms per heart cycle. By combining these palpograms, one compound palpogram per heart cycle is determined (25). In a recent study in humans, 3D palpograms were derived from continuous intravascular ultrasound pullbacks of entire coronary arteries. Patients ($n = 55$) were classified by clinical presentation as having stable angina, unstable angina, or acute myocardial infarction (AMI). In every patient, one coronary artery was scanned (culprit vessel in stable and unstable angina, nonculprit vessel in AMI) and the number of deformable plaques was assessed. Stable angina patients had significantly fewer deformable plaques per vessel (0.6 ± 0.6) than unstable angina patients (1.6 ± 0.7) ($p < 0.0019$) or AMI patients (2.0 ± 0.7) ($p < 0.0001$). Levels of C-reactive protein positively correlated with the number of mechanically deformable plaques ($R^2 = 0.65$; $p < 0.0001$) (26).

Strain measurements give an indication of the mechanical properties of the plaque without taking into account the shear forces, which may be responsible for activation of biologic processes that induce instabilities. Assessment of shear stress is feasible by obtaining high-resolution reconstruction of 3D coronary lumen and wall morphology using the combination of angiography and IVUS (27). Briefly, a biplane angiogram of a sheath-based IVUS catheter taken at end-diastole allows reconstruction of the 3D pullback trajectory of the catheter. Combining this path with lumen and wall information derived from IVUS images that are successively acquired during catheter pullback at end-diastole gives accurate 3D lumen and wall reconstruction with a resolution determined by IVUS. Filling the 3D lumen space with high-resolution 3D grit allows calculation of the detailed blood velocity profile in the lumen (28). For this purpose, absolute flow and blood viscosity need to be provided as boundary conditions. From the blood velocity profile, local wall shear stress on the endothelium can be accurately calculated. Wall shear stress is the frictional force, normalized to surface area, that is induced by the blood passing the wall. Although from a mechanical point of view shear stress is of a very small magnitude compared with blood pressure-induced tensile stress it has a profound influence on vascular biology (29) and explains the localization of atherosclerotic plaque in the presence of systemic risk factors (30). Many of these biologic processes also

influence the stability of the vulnerable plaque, including inflammation, thrombogenicity, vessel remodeling, intimal thickening or regression, and smooth muscle cell proliferation. Therefore, the assessments of shear stress in combination with strain measurements will unravel significant pathophysiologic aspects of plaque vulnerability.

CONCLUSIONS

Both in vitro and in vivo studies have revealed that strain is higher in fatty than in fibrous plaques. Additionally, the presence of a high-strain region has a high sensitivity and specificity to detect the vulnerable plaque. High-strain spots correlate with clinical symptoms and inflammation markers. The presence of a high-strain spot that is surrounded by low strain has a high predictive power to identify the rupture-prone plaque in vitro with high sensitivity and specificity. Intravascular palpography is a technique that assesses the local strain of the vessel wall and plaque, and can therefore be applied in patients to assess the vulnerability of plaques. Three-dimensional palpography allows the identification of weak spots over the full length of a coronary artery. A prospective study in patients that correlates clinical events with the distribution of these weak spots is currently being performed. Because palpography only requires ultrasound data sets that are acquired at different levels of intraluminal pressure, it can be realized using conventional clinically used catheters.

Reprint requests and correspondence: Dr. Johannes A Schaar, Experimental Echocardiography Ee23.02, Erasmus Medical Center, PO Box 1738, 3000DR Rotterdam, the Netherlands. E-mail: j.schaar@erasmusmc.nl.

REFERENCES

1. Loree HM, Kamm RD, Stringfellow RG, et al. Effects of fibrous cap thickness on peak circumferential stress in model atherosclerotic vessels. Circ Res 1992;71:850–8.
2. Richardson PD, Davies MJ, Born GVR. Influence of plaque configuration and stress distribution on fissuring of coronary atherosclerotic plaques. Lancet 1989;21:941–4.
3. Lendon CL, Davies MJ, Born GVR, et al. Atherosclerotic plaque caps are locally weakened when macrophage density is increased. Atherosclerosis 1991;87:87–90.
4. Céspedes EI, de Korte CL, van der Steen AFW. Intraluminal ultrasonic palpation: assessment of local and cross-sectional tissue stiffness. Ultrasound Med Biol 2000;26:385–96.
5. Mintz GS, Nissen SE, Anderson WD, et al. ACC clinical expert consensus document on standards for acquisition, measurement and reporting of intravascular ultrasound studies (IVUS). A report of the American College of Cardiology Task Force on Clinical Expert Consensus Documents. J Am Coll Cardiol 2001;37:1478–92.
6. Prati F, Arbustini E, Labellarte A, et al. Correlation between high frequency intravascular ultrasound and histomorphology in human coronary arteries. Heart 2001;85:567–70.
7. Komiyama N, Berry G, Kolz M, et al. Tissue characterization of atherosclerotic plaques by intravascular ultrasound radiofrequency signal analysis: an in vitro study of human coronary arteries. Am Heart J 2000;140:565–74.
8. Hiro T, Fujii T, Yasumoto K, et al. Detection of fibrous cap in atherosclerotic plaque by intravascular ultrasound by use of color mapping of angle-dependent echo-intensity variation. Circulation 2001;103:1206–11.
9. Loree HM, Tobias BJ, Gibson LJ, et al. Mechanical properties of model atherosclerotic lesion lipid pools. Arterioscler Thromb Vasc 1994;14:230–4.
10. Loree HM, Grodzinsky AJ, Park SY, et al. Static circumferential tangential modulus of human atherosclerotic tissue. J Biomech 1994; 27:195–204.
11. Lee RT, Richardson G, Loree HM, et al. Prediction of mechanical properties of human atherosclerotic tissue by high-frequency intravascular ultrasound imaging. Arterioscler Thromb Vasc 1992;12:1–5.
12. Cheng GC, Loree HM, Kamm RD, et al. Distribution of circumferential stress in ruptured and stable atherosclerotic lesions. A structural analysis with histopathological correlation. Circulation 1993;87:1179–87.
13. Céspedes EI, Ophir J, Ponnekanti H, et al. Elastography: elasticity imaging using ultrasound with application to muscle and breast in vivo. Ultrason Imaging 1993;17:73–88.
14. Ophir J, Céspedes EI, Ponnekanti H, et al. Elastography: a method for imaging the elasticity in biological tissues. Ultrason Imag 1991;13: 111–34.
15. Céspedes EI, Huang Y, Ophir J, et al. Methods for estimation of subsample time delays of digitized echo signals. Ultrason Imag 1995;17: 142–71.
16. Sarvazyan AP, Emelianov SY, Skovorada AR, inventors; Medical Biophysics International, assignee. Intracavity device for elasticity imaging. U.S. patent 5265612. November 30, 1993.
17. de Korte CL, Pasterkamp G, van der Steen AFW, et al. Characterization of plaque components using intravascular ultrasound elastography in human femoral and coronary arteries in vitro. Circulation 2000;102:617–23.
18. Lee RT, Richardson G, Loree HM, et al. Prediction of mechanical properties of human atherosclerotic tissue by high-frequency intravascular ultrasound imaging. Arterioscler Thromb Vasc 1992;12:1–5.
19. Schaar JA, de Korte CL, Mastik F, et al. Characterizing vulnerable plaque features with intravascular elastography. Circulation 2003;108:2636.
20. de Korte CL, Sierevogel M, Mastik F, et al. Identification of atherosclerotic plaque components with intravascular ultrasound elastography in vivo: a Yucatan pig study. Circulation 2002;105: 1627–30.
21. de Korte CL, Carlier SG, Mastik F, et al. Morphological and mechanical information of coronary arteries obtained with Intravascular elastography: a feasibility study in vivo. Eur Heart J 2002;23:405–13.
22. de Korte CL, Doyley MM, Carlier SG, et al. High resolution IVUS elastography in patients. In: IEEE Ultrasonics Symposium, Puerto Rico, 2000. New York, NY: IEEE, 2000:1767–70.
23. Konofagou E, Ophir J. A new elastographic method for estimation and imaging of lateral displacements, lateral strains, corrected axial strains, and Poisson's ratios in tissues. Ultrasound Med Biol 1998;24: 1183–99.
24. Kallel F, Ophir J. Three dimensional tissue motion and its effect on image noise in elastography. IEEE Trans Ultrason Ferroelectr Freq Control 1997;44:1286–96.
25. Doyley M, Mastik F, de Korte CL, et al. Advancing intravascular ultrasonic palpation towards clinical applications. Ultrasound Med Biol 2001;27:1471–80.
26. Schaar JA, Regar E, Mastik F, et al. Incidence of high-strain patterns in human coronary arteries: assessment with three-dimensional intravascular palpography and correlation with clinical presentation. Circulation 2004;109:2716–9.
27. Slager CJ, Wentzel JJ, Schuurbiers JCH, et al. True 3-dimensional reconstruction of coronary arteries in patients by fusion of angiography and IVUS (ANGUS) and its quantitative validation. Circulation 2000;102:511–6.
28. Thury A, Wentzel JJ, Schuurbiers JC, et al. Prominent role of tensile stress in propagation of a dissection after coronary stenting: computational fluid dynamic analysis on true 3D-reconstructed segment. Circulation 2001;104:E53–4.
29. Malek AM, Alper SL, Izumo S. Hemodynamic shear stress and its role in atherosclerosis. JAMA 1999;282:2035–42.
30. Asakura T, Karino T. Flow patterns and spatial distribution of atherosclerotic lesions in human coronary arteries. Circ Res 1990;66:1045–66.